Low humidity dependence of proton conductivity in modified zirconium (IV)-hydroxy ethylidene diphosphonates

Takaya Ogawa,[1,†,*] Gopinathan M. Anilkumar,[1,2] Takanori Tamaki,[1] Hidenori Ohashi,[1,‡] Takeo Yamaguchi[1,*]

[1]*Laboratory for Chemistry and Life Science, Institute of Innovative Research, Tokyo Institute of Technology, Nagatsuta 4259, Midori-ku, Yokohama 226-8503, Japan*

[2]*Research & Development Center, Noritake, Co., Ltd., 300 Higashiyama, Miyoshi-cho, Miyoshi, Aichi 470-0293, Japan*

[†]*presemt address: Department of Socio-Environmental Energy Science, Graduate School of Energy Science, Kyoto University, Yoshida-Honmachi, Sakyo-ku, Kyoto 606–8501, Japan.*

[‡]*presemt address: Department of Chemical Engineering, Tokyo University of Agriculture and Technology, 2-24-16 Naka-cho, Koganei, Tokyo 184-8588, Japan*

[*]Author to whom correspondence to be addressed. Electronic mail: ogawa.takaya.8s@kyoto-u.ac.jp (T. O.); yamag@res.titech.ac.jp (T. Y.)

Abstract

Proton conducting materials play an essential role in various fields of science and many applications, such as polymer electrolyte fuel cells (PEFCs). However, their proton conductivities suffer from the strong dependence on relative humidity (RH) and severely decrease at low RH conditions. Here, we synthesized zirconium (IV)-hydroxy ethylidene diphosphonates (ZrHEDP), which have phosphonic acid groups at a close distance. As the acidic groups are more concentrated in ZrHEDP, the proton conductivity exhibits lower dependence on the RH. In particular, the ZrHEDP with the largest amount of phosphonic acid groups among the examined samples

showed the lowest RH dependence; the proton conductivity at 40% RH remained 2/3 of the conductivity at 95% RH, whereas a representative electrolyte, Nafion, at 40 % RH showed 1/5-1/20 of its conductivity at 95% RH.

1. Introduction

Proton conduction in materials is an essential phenomenon in various systems, such as polymer electrolyte fuel cells (PEFCs), where the proton conductivity of the electrolyte plays a major role in determining the overall performance of the PEFC system.[1-3] PEFC is an efficient electricity generator without CO_2 emission in operation, mainly applied for the energy source of fuel cell vehicles (FCVs). Looking at the broad commercialization and cost reduction of FCVs, the operation under high temperature is essential for catalyst materials to enhance activity and eliminate poisoning by impurities in the fuel and for radiators and water management systems to be simplified.[4] However, the proton conductivities severely diminish at low relative humidity (RH) conditions.[2, 3] At high temperatures, fast drying of the electrolyte results in decreased conductivity and a huge ohmic loss. Hence, the severe dependence of proton conductivity on RH imposes the limitation of upper temperature (approximately 80 °C) during the operation of PEFC. Many efforts have been made to overcome the reliance on RH and have achieved some successes,[2, 5-8] but it remains the issue, especially at high temperatures.

This serious proton conductivity dependence on RH is explained by the inevitable characteristic of the conventional proton conduction mechanisms: the vehicle mechanism and the structural diffusion.[9, 10] In the vehicle mechanism, a proton transfers as H_3O^+ via molecular diffusion. Structural diffusion is typically regarded to be the same as the well-known "the Grotthus mechanism." The structural diffusion involves necessary coordination constructed by the following two procedures: "hopping," in which a proton hops from a proton

donor to an acceptor along a hydrogen bond (H-bond), and "reorientation," in which a H-bond is cleaved, and the proton reorients to another proton acceptor.[11-15] The diffusion occurs through coordination originating from reorientation in the second hydration shell, followed by successive hopping events involving the movement of $H_5O_2^+$ (the Zundel cation) and $H_9O_4^+$ (the Eigen cation), with several water molecules per proton.[12-17] The rate-determining step is the reorientation[10, 18] The movement of water molecules is indispensable because a thermal fluctuation of water breaks a H-bond to cause reorientation.[13, 19] Obviously, water movement is also essential for the vehicle mechanism. Therefore, both mechanisms inevitably require water movements, and thus water molecules (i.e., high RH condition) are crucial.

Meanwhile, the "packed-acid mechanism" has been recently proposed as a derivative of Grotthuss mechanisms that occurs in materials consisting of concentrated acids.[15, 20] In the packed-acid mechanism, acid-acid interactions weaken H-bonds and stimulate reorientation.[21] Thus, the mechanism does not require water molecule movements. In fact, the proton in the material comprising of packed-acids diffuses even when water is frozen, whereas an ordinary proton conducting material cannot retain the proton diffusivity under the same condition.[15, 20] It suggests that the packed-acid mechanism might not be strongly influenced by RH.

The *ab initio* calculation showed that the suitable acid group to induce the packed-acid mechanism is a hydrocarbon-based phosphonic acid group rather than a sulfonic acid group, generally employed for electrolytes in PEFCs due to its high dissociation constant of a proton.[22] Based on the theoretical suggestion, the distance between hydrocarbon-based phosphonic acid groups is preferably ~13Å to induce the packed-acid mechanism.[22] There have been many studies on polymers functionalized with dense-phosphonic acid groups.[23-25] However,

polymers are generally flexible and swollen by water under humid conditions, making it challenging to maintain a high-density acid structure.

On the other hand, inorganic materials with a rigid framework, such as zirconium phosphonates, possess high stability toward swelling and keep the densified acidic circumstance. Moreover, zirconium phosphonates have a 2D structure and can consist of acid groups at a certain distance, 4.5−5.5 Å continuously along the layer (Fig. 1a).[26-29] There is no research to regulate phosphonic acid groups at such a close distance and examine the humidity dependence of the electrolyte.

In this study, we synthesized zirconium (IV)-hydroxy ethylidene diphosphonates (ZrHEDPs) to investigate whether the reliance of proton conductivity on RH can be overcome by making the close distance between phosphonic acid groups. ZrHEDP has hydrocarbon-based phosphonic acid groups, -$C(OH)CH_3$-PO_3H_2, and the average distance between the acid moiety was controlled by synthesis conditions. ZrHEDP is one of the best electrolytes to demonstrate the objective due to its rigid structure and property of having acidic groups at a close distance.

2. Experimental

2.1 Material preparation

The synthesis of ZrHEDP was carried out as follows. At first, nano-zirconia precursor powder (Zr-precursor) was prepared by a method reported earlier by our group.[30] One gram of the synthesized Zr-precursor powder was dispersed in 25 ml of 1 M HNO_3 (Solution A). Next, the required amounts of 1-hydroxy-1,1-ethylidene diphosphonic acid (HEDP, H_2PO_3-$C(OH)CH_3$-PO_3H_2) (Fig. 1b) (Strem Chemicals, 95%) were dissolved in

12.5g of distilled water, followed by heating at 50 °C for 30 minutes (Solution B). Next, both heated solutions (Solution A and B) were mixed at 50 °C and kept stirring for 4 hours, then heated at 70 °C for 4.5 hours in a sealed vessel. Finally, the obtained precipitate was dried at 90 °C, followed by washing with water until neutral pH was attained. HEDP/Zr-precursor ratio (weight) was varied (0.65, 0.90, 1.10, and 1.30) to synthesize ZrHEDPs functionalized with the different amounts of phosphonic acid group, *i.e.*, the several average distances between acid moieties. We labeled ZrHEDP samples by their mole ratio of phosphorous per zirconium (P/Zr). The other synthesis conditions and P/Zr results are shown in Section I of Supplementary information for reproducibility.

Figure 1 (c), (d), and (e) show the schematic representation of the 2D structures of ZrHEDP with P/Zr = 2, 3, and 4, respectively, which we expected to synthesize by the above method. In the structure with P/Zr = 2, both phosphonic acids in HEDP were introduced into the Zr-O-network layer and lost the ability to dissociate proton (Fig. 1(c)). On the other hand, in the structure with P/Zr = 4, one phosphonic acid was fixed in Zr-O-network, and the other phosphonic acid remained movable and titratable (-PO_3H_2) (Fig. 1(e)). The ZrHEDP sample can include both structures with P/Zr = 2 and 4. If there is no unreacted and remaining HEDP in the ZrHEDP samples, the ratio of the structure with P/Zr = 4 is estimated as follows:

$$P/Zr = \left(P/Zr\ of\ Fig.1(c)\right) \times (1-x) + \left(P/Zr\ of\ Fig.1(e)\right) \times x = 2 \times (1-x) + 4 \times x \quad (1)$$

$$x = (P/Zr - 2)/2 \quad (2)$$

where x is the ratio of the structure with P/Zr = 4. Then, the value of "(P/Zr – 2)/2 × 100 (%)" represents the minimum ratio of -PO_3H_2 per whole phosphonate site, while why the ratio is the "minimum" is because there is

a possibility of remaining ZrO_2. Thus, P/Zr = 3.0 indicates that more than 50% of entire phosphonate sites are -PO_3H_2 (Fig. 1(d)), *i.e.*, one of every two phosphonate sites in the Zr-O-network is -PO_3H_2, and the other is immobilized -PO_3-. Therefore, we expected that the higher P/Zr means a closer distance between -PO_3H_2.

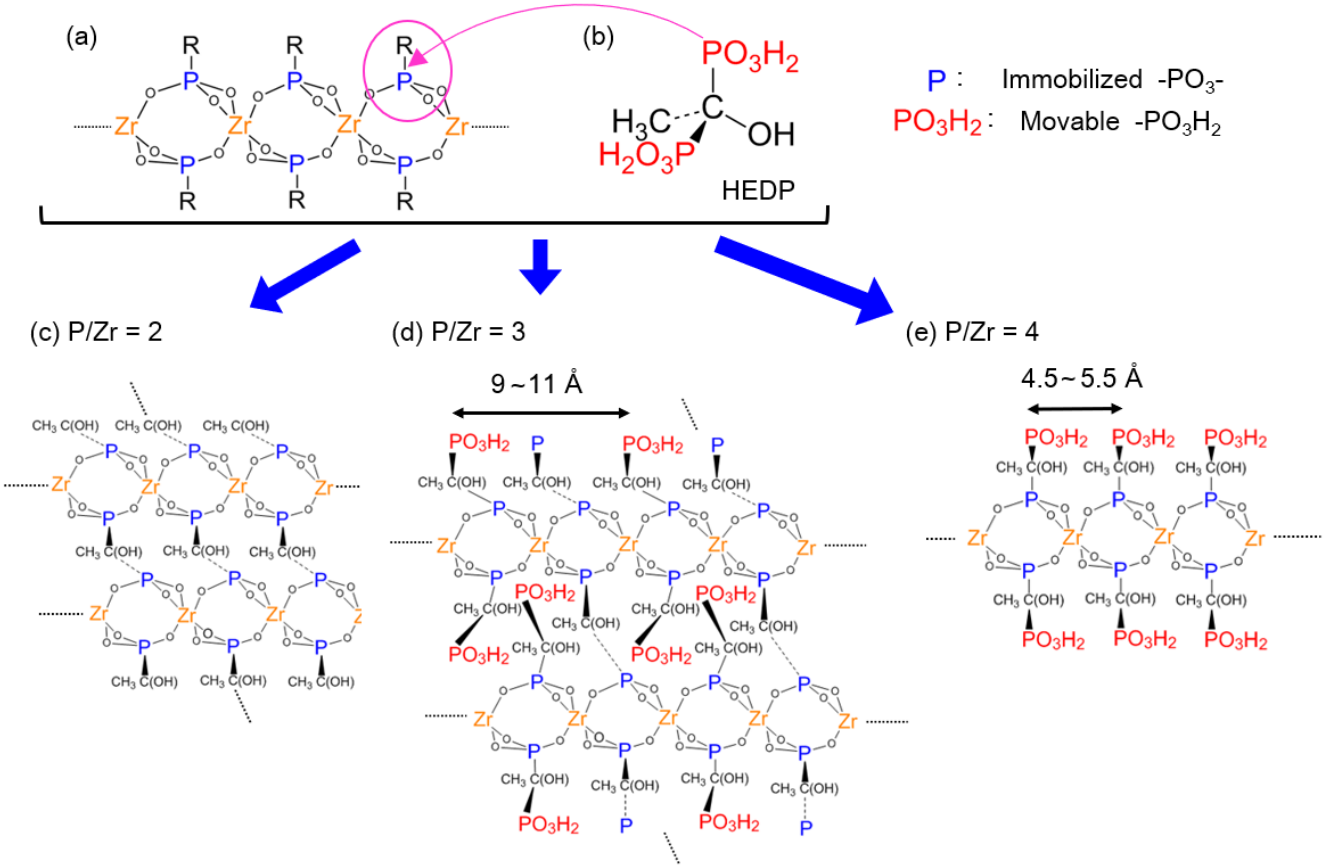

Figure 1 Schematic representation of various ZrHEDP structures. **a)** model of $Zr(PO_3\text{-}R)_2$, **b)** HEDP, **c)** $Zr(PO_3)_2C(OH)CH_3$, **d)** $Zr(PO_3\text{-}C(OH)CH_3\text{-}PO_3H_2)(PO_3\text{-}C(OH)CH_3)$, **e)** $Zr(PO_3\text{-}C(OH)CH_3\text{-}PO_3H_2)_2$

2.2 Characterization

Inductively coupled plasma atomic emission spectroscopy (ICP–AES) was employed to measure the element weights and ratios of the samples using ICPS-8100 (Shimadzu). The ^{31}P solid-state magic angle spinning nuclear magnetic resonance (MAS-NMR) spectra were measured with JEOL-JNM-ECA-600MHz (Frequency: 242.95MHz, relaxation delay: 5s, contact time: 2ms, scans: 1000). Fourier Transform Infrared Spectroscopy

(FT–IR) spectra were obtained with an FT–IR-6200 (Jasco Co., Ltd.) spectrophotometer. X-ray Diffraction (XRD) analyses were carried out with RINT2000 (Rigaku Co., Ltd.) using a Cu Ka X-ray source at 40 kV and 40 mA. Differential scanning calorimetry (DSC) was analyzed with Perkin Elmer DSC-7 purchased from PerkinElmer Japan Co., Ltd after incubation of samples at 100% RH for three days. Proton conductivity values were measured using the two-probe alternative current impedance method with a Solartron 1260 Impedance/Gain Phase Analyzer in the frequency range of 1–32 MHz and at a signal amplitude of 100 mV.

3. Results

3.1 Characterizations of ZrHEDP structures

ICP−AES measurement was utilized to confirm that the P/Zr values of ZrHEDP samples were 1.8, 2.5, 2.8, and 3.0, synthesized in the condition that the HEDP/Zr-precursor ratio (weight) were 0.65, 0.90, 1.10, and 1.30, respectively. We utilized these P/Zr values for labeling the samples.

The broad XRD peaks (Fig. 2(a)), observed in the two theta range 18-35°, indicated the amorphous nature of the materials.[31]

^{31}P solid-state MAS NMR spectra of HEDP and the ZrHEDPs with different P/Zr ratios are shown in Fig. 2(b). In the ZrHEDP spectra, the main peak was observed at approximately 13 ppm and a shoulder peak near 3 ppm. The intensity of peaks at 3 ppm became stronger as the value of the P/Zr ratio increased.

FT-IR spectra of ZrHEDP samples are presented in Fig. S1 and are confirmed as the same as ZrHEDPs in previous reports.[32] Figure 2(c) represents the FT-IR spectra of the synthesized ZrHEDPs around approximately 1060 cm^{-1} due to PO_3 stretching (P–O).[33] As for the spectra of the ZrHEDP with higher P/Zr values, the P–O

shifted to higher wavenumbers. The wavenumbers of the P–O in the ZrHEDP with P/Zr = 1.8, 2.5, 2.8, and 3.0 were 1052, 1058, 1058, and 1061 cm^{-1}, respectively.

DSC analysis was performed on ZrHEDP samples (Fig. 2(d)). DSC results showed that the freezing point decreased as the P/Zr ratio increased. The freezing points of the ZrHEDPs with P/Zr = 1.8, 2.5, 2.8, and 3.0 were –1.5, –1.8, –2.5, and –3.3 °C, respectively.

These results will be interpreted and discussed in Section 4.1.

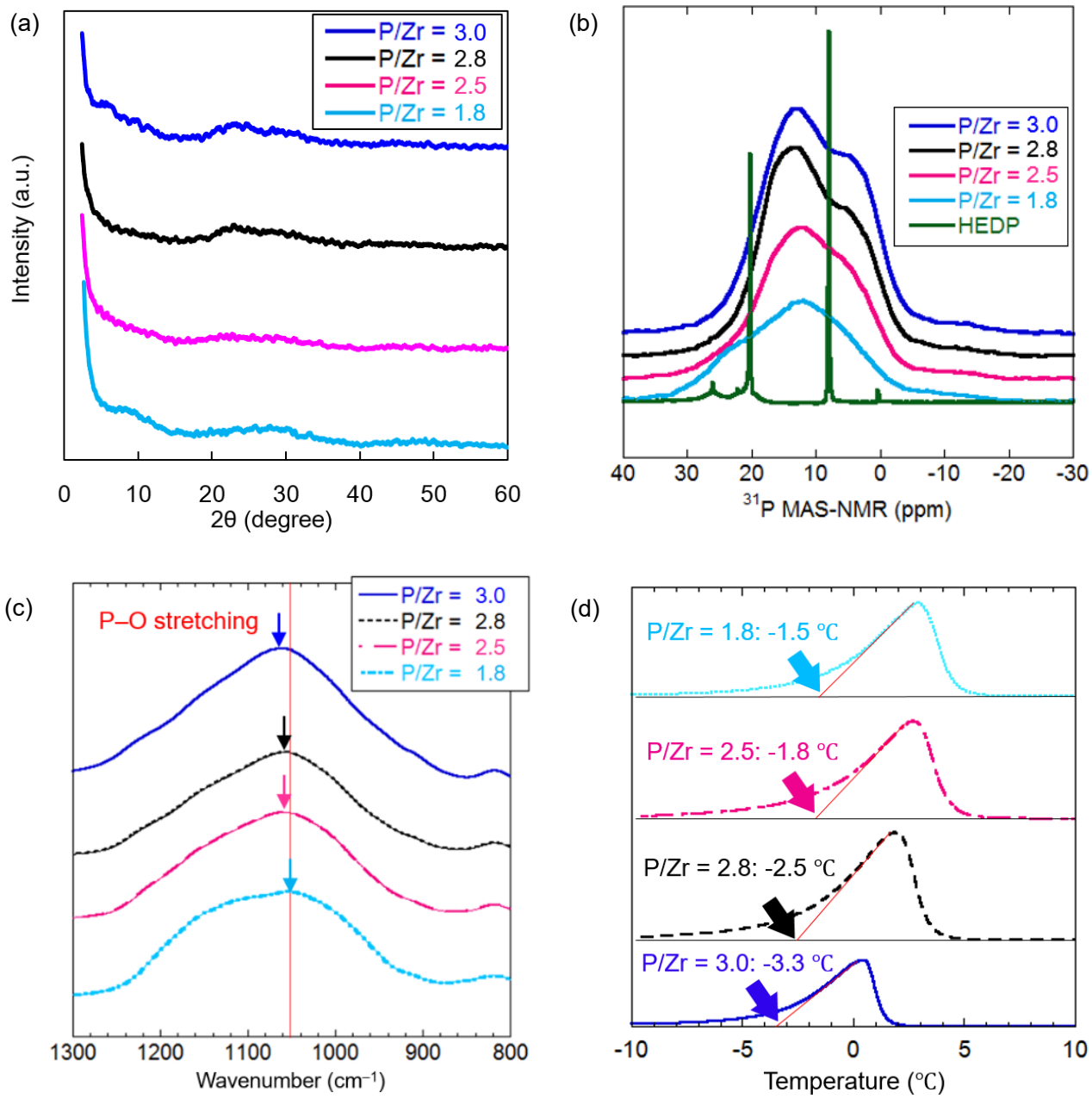

Figure 2 (a) XRD spectra (b) ^{31}P solid-state MAS-NMR spectra (c) FT-IR spectra focusing on the P–O stretching peak position (d) DSC results and freezing point of adsorbed water in ZrHEDP

3.2 Proton conductivity and dependence on RH

Proton conductivities of the ZrHEDP powders were measured at various RH conditions (Fig. 3) as pellet samples (diameter: 13 mm, thickness: ~0.1 mm), made by uniaxial pressing the respective powders. Figure 3 shows the enhanced proton conductivity values and low dependence on RH in ZrHEDP with a high P/Zr ratio (see Fig. S2 for cole-cole plots). In particular, the proton conductivity of the ZrHEDP pellet with P/Zr = 3.0 at 95% RH only decreased to 2/3 at 40% RH. On the other hand, Nafion at 40% RH exhibits 1/5-1/20 of the proton conductivity compared to its value at 95% RH.[34, 35] Hence, the dependence on RH in the synthesized ZrHEDP is low. The E_a of the ZrHEDP pellet with P/Zr = 3.0 was 15.3–35.4 kJ/mol at 95% RH and 90 °C (see Fig. S3). The origin of these conductivities will be discussed in Section 4.2.

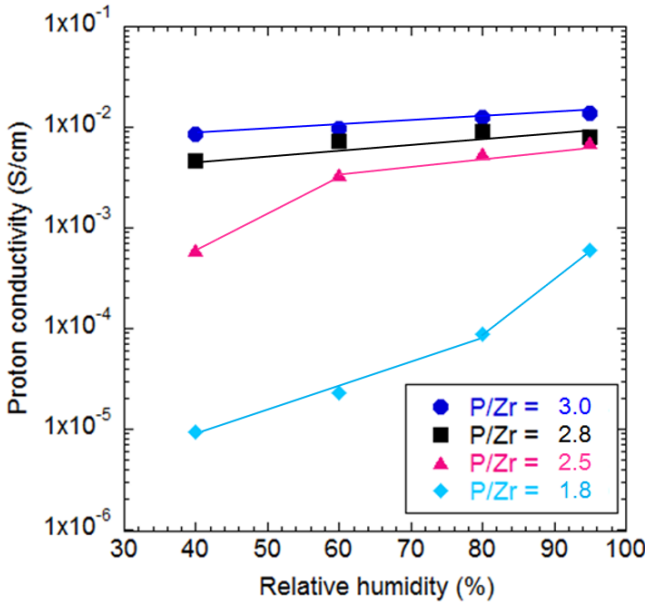

Figure 3 Proton conductivity data of the ZrHEDP with different P/Zr ratios at 90 °C.

4. Discussion

4.1 The structure of the ZrHEDP samples

XRD results indicated all of the ZrHEDP samples are in amorphous states. On the other hand, the centre carbon bound to two phosphorous in HEDP has a sp^3 hybrid orbital, twisting the whole HEDP structure. It eventually disturbs keeping the layer-by-layer structure,[36] which could be the origin of the amorphous state. In this case, it is difficult for both phosphoric acid groups of HEDP to be fixed in zirconium layers due to steric hindrance, and either of the two readily becomes movable -PO_3H_2.

As shown in Fig. 2(a), the peaks in the range 2θ = 5–12° (≈ 7–18 Å) in the XRD patterns were unclear, generally considered the distances for ZrP layers.[37] The broad peaks around 2θ = 18–35° (≈ 3–5 Å) were identified and should be derived from the Zr-Zr distance (= 4.5–5.5 Å, indicated in Fig. 1(e))[26-29] because the atomic scattering factor of Zr is much higher than other elements in ZrHEDP (H, C, O, and P). Therefore, ZrHEDPs do not have the layer-by-layer structure but have the 2D structure, even though the plane is not so continuous because of the quite broadness of the peak. The near Zr-Zr proximity on the 2D plane is sufficient to make the distance among -PO_3H_2s close along the plane.

ICP-AES results showed that the P/Zr of the ZrHEDP samples ranged from 1.8 to 3.0. With the speculation of the schematically represented structure in Fig. 1(c)-(e), the ZrHEDP samples are composed of the composite structure of P/Zr = 2 (Fig. 1(c)) and 4 (Fig. 1(e)) with some unreacted zirconia precursor. If phosphonic acid groups in HEDP were not captured in Zr layers, unreacted HEDP should be eliminated in the washing process

by water (see methods) because HEDP is water-soluble. Hence, as the P/Zr ratio increases, more phosphonic acid groups should be attached to Zr layers, as shown in Fig. 1(e).

As for NMR results (Fig. 2(b)), all peaks in ZrHEDP samples are broad compared to those in HEDP. The broadness indicated that all phosphonic acid groups are immobile and fixed to Zr layers,[38] and thus no free HEDP remained in ZrHEDP samples. The specific assignment for ^{31}P peaks in ZrHEDP is more complex than the corresponding bands for other zirconium phosphonates, such as biphenylene-bisphosphonates, likely due to the angular nature of the ether-bisphosphonate unit, which imposes two different orientations with the inorganic layer.[36] Nevertheless, the peak of the more freely movable ^{31}P atom was expected to shift to a lower field.[39, 40] Therefore, the peaks at 3 and 13 ppm can be attributed to the movable -PO_3H_2 and the immobilized -PO_3- in the Zr-O-network layer, respectively. Furthermore, the intensity of peaks at 3 ppm became stronger as the value of the P/Zr ratio increased. Therefore, these results suggested that ZrHEDP with a higher P/Zr value contains a lot of -PO_3H_2 moieties, which matches the above indications from the ICP–AES results. These two results mean that ZrHEDP samples have the mixture of structures illustrated in Fig. 1(c)-(e), and the large amount of -PO_3H_2 moieties existed in the ZrHEDP with high P/Zr.

FT-IR results showed that P–O vibration in the ZrHEDP shifts to high wavenumbers when the P/Zr is large (Fig. 2(c)). A higher wavenumber for the P–O indicates a higher energy state, *i.e.*, a more unstable bond of -PO_3H_2.[41] It is identical to the case that the H-bond is weakened by acid-acid interactions.[15, 41] The acid-acid interaction does not originate if acids do not concentrate to some extent.[21, 22] Then, the large amounts of -PO_3H_2 were densified enough to generate acid-acid interactions. DSC results also showed the same tendency because

ZrHEDPs with a higher P/Zr exhibited a lower freezing temperature (Fig. 2(d)). Generally, the freezing point is reduced when the water is firmly bound to other groups.[42, 43] Concentrated acids can bind water molecules intensely because multiple acids can form H-bonds to a single water molecule.[44] Therefore, the decrease of freezing point in ZrHEDP should be originated from the densified -PO_3H_2.

In summary, even though XRD results indicated that the ZrHEDP samples were amorphous states and no clear peaks for the layer-by-layer structure, the peaks for Zr-Zr distance were detected, which is more critical than the layer-by-layer structure to retain the -PO_3H_2 close. Furthermore, ICP–AES and NMR results suggested a larger amount of -PO_3H_2 as P/Zr increases. Furthermore, as the essential insights, FT-IR and DSC results identified the interaction of -PO_3H_2 in close proximity. These results indicate that ZrHEDP with high P/Zr has a lot of -PO_3H_2 at a close distance to interact with each other.

4.2 Proton conductivity of ZrHEDPs with dense-PO_3H_2 moieties

The proton conductivity data (Fig. 3) shows that the ZrHEDP samples with a high P/Zr ratio have low dependence on RH. It is the same tendency with the previous reports on sulfonated aromatic hydrocarbon polymers.[6, 8, 45] The proton conductivity in this kind of random copolymer is more dependent on RH than that of Nafion.[2] However, their humidity reliance is mitigated by introducing a large amount of sulfuric acid group to a polymer, and the humidity dependence becomes comparable to that of Nafion.[8, 45] The properties deriving from concentrated acids seem to trigger the low dependence.

As one of the plausible explanations, the packed-acid mechanism might be the origin of the low dependence, described in the following. As introduced in Section 1 in detail, the conventional mechanism of proton

conduction must require water movements.[9, 10] The inevitable characteristic leads the severe dependence on RH. On the other hand, the packed-acid mechanism, which occurs among concentrated acids, facilitates proton conductions without water movements.[15, 20] It means that the proton conduction via the packed-acid mechanism has the potential to be influenced not extensively by water, *i.e.*, RH.

Here, we investigated whether the average distances among phosphonic acid groups in the ZrHEDP samples were concentrated to facilitate the packed-acid mechanism by comparing them with the theoretical suggestion in our previous report.[22] Based on the results discussed in Section 4.1, the ZrHEDP samples include not only the structure in Fig. 1(c) but also Fig. 1(d)-(e). The distance between -PO_3H_2s is 9~11 Å in the structure of Fig. 1 (d), along with the zirconium phosphonate layer. The distance is estimated by -PO_3H_2 concentrations based on ICP-AES results and the volume and weight of the pellets for proton conductivity measurement (See Section 3.2 and Section III in Supplementary Information for more detailed methods). The average distances are 7.4, 9.0, and 10.7 Å for P/Zr = 3.0, 2.8, and 2.5, respectively. Our theoretical material design proposed that the hydrocarbon-based phosphonic acid moieties are better to exist at a close distance (~13 Å) to facilitate the packed-acid mechanism.[22] The estimated average lengths of -$C(OH)CH_3$-PO_3H_2 in ZrHEDP samples are within the suggested range. In addition, the theoretical results indicated that the frequency of the mechanism increases gradually as the distance between acids becomes close.[22] Thus, the gradual change of the RH dependence associated with the P/Zr is also explained by the theoretical insights. The ZrHEDP samples with P/Zr = 2.5 and 1.8 show higher dependence on RH as P/Zr decreases. In these samples with low P/Zr, other mechanisms, such as structural diffusion or vehicle mechanism, seem to be dominant, and the packed-acid mechanism is not (these

mechanisms can occur in parallel).

Furthermore, the low freezing temperatures in DSC results indicate that water in ZrHEDP is less movable as P/Zr increases, not favorable for conventional mechanisms of proton conduction. Nevertheless, the proton conductivity of the ZrHEDP with high P/Zr is enhanced, which also supports that the proton conduction mechanism in the ZrHEDP samples is the packed-acid mechanism. In addition, the E_a of the ZrHEDP pellet with P/Zr = 3.0 was measured to be 15.3–35.4 kJ/mol at 95% RH and 90 °C. These values are below 0.4 eV (= 38.6 kJ/mol), typically considered the E_a of the Grotthus mechanism.[46] The E_a of the previous sample where proton moves through packed-acid mechanism exhibited 41 kJ/mol.[20] It also means that the proton conduction mechanism in ZrHEDP samples can be the packed-acid mechanism. Therefore, it is possible that the low dependence on RH originated from the concentrated -PO_3H_2s through the packed-acid mechanism.

As shown in Table S1 in Supplementary Infomation, we could not obtain ZrHEDP with P/Zr > 3. HEDP, where both phosphonic acid groups are immobilized as -PO_3 in ZrHEDP with P/Zr = 2, can bridge two ZrHEDP layers. Therefore, ZrHEDP with P/Zr > 3 will have fewer "bridging-HEDPs," resulting in more open space for water adsorption and less packed-PO_3H_2s. Therefore, if the appropriate synthesis (or washing) condition leads to the P/Zr > 3, that sample might have strong RH dependence. In addition, an excessive amount of -PO_3H_2 in ZrHEDP with P/Zr > 3 might induce overly hydrophilic properties, which can be the reason to be washed out and not exceed P/Zr = 3 (see Section I in Supplementary information).

The proton conductivity values of the best ZrHEDP sample (P/Zr = 3.0) were around 0.01 S/cm at broad RH condition, 40-95%, and promisingly showed low dependence on RH. However, 0.01 S/cm is not adequate for

practical application in PEFC, while Nafion has 0.1 S/cm at 90% RH condition.[34, 35] It is because phosphonic acid groups have a lower dissociation constant of proton than sulfonic acid groups. Therefore, if the pKa of the -PO_3H_2 is enhanced by some methods (e.g., introducing an electron-withdrawing element), it is possible to obtain the material with low dependence on RH and enough proton conductivity for the PEFC operation.

5. Conclusion

ZrHEDPs, zirconium phosphonate functionalized with -PO_3H_2s moieties, were synthesized to overcome the humidity dependence of proton conductivity, the serious drawback of proton conducting materials. As the P/Zr in ZrHEDPs increased, they had more packed-PO_3H_2 moieties and exhibited a higher proton conductivity with a lower reliance on RH. Notably, the proton conductivity of the ZrHEDP pellet with P/Zr = 3.0 at 95% RH only decreased to 2/3 at 40% RH, whereas Nafion at 40 % RH shows 1/5-1/20 of its conductivity at 95% RH. The low RH dependence is an ideal property for several applications, such as PEFC applications.

Supplementary Information: The several synthesis conditions and the ICP-AES results, FT-IR spectra for all samples, cole-cole plots of proton conductivity measurements, Arrhenius plots, and the detailed method estimating the average distance between -PO_3H_2 moieties in ZrHEDP samples

Acknowledgment: Part of this paper is based on results obtained from a project, JPNP20003, commissioned by the New Energy and Industrial Technology Development Organization (NEDO). The authors acknowledge the fruitful advice of Prof. Keiichi N. Ishihara on XRD results and the assistance of Dr. Toshiyuki Yokoi and Dr. Yoshiyuki Nakamura with the solid-state ^{31}P MAS NMR measurements.

References

1. T. Ogawa, M. Takeuchi and Y. Kajikawa, Comprehensive Analysis of Trends and Emerging Technologies in All Types of Fuel Cells Based on a Computational Method, *Sustainability*, 2018, **10**, 458.
2. D. W. Shin, M. D. Guiver and Y. M. Lee, Hydrocarbon-Based Polymer Electrolyte Membranes: Importance of Morphology on Ion Transport and Membrane Stability, *Chem Rev*, 2017, **117**, 4759-4805.
3. C. H. Park, S. Y. Lee, D. S. Hwang, D. W. Shin, D. H. Cho, K. H. Lee, T. W. Kim, M. Lee, D. S. Kim, C. M. Doherty, A. W. Thornton, A. J. Hill, M. D. Guiver and Y. M. Lee, Nanocrack-regulated self-humidifying membranes, *Nature*, 2016, **532**, 480-483.
4. V. Di Noto, T. A. Zawodzinski, A. M. Herring, G. A. Giffin, E. Negro and S. Lavina, Polymer electrolytes for a hydrogen economy, *Int. J. Hydrog. Energy*, 2012, **37**, 6120-6131.
5. V. Di Noto, M. Piga, G. A. Giffin, K. Vezzu and T. A. Zawodzinski, Interplay between Mechanical, Electrical, and Thermal Relaxations in Nanocomposite Proton Conducting Membranes Based on Nafion and a $[(ZrO_2)\cdot(Ta_2O_5)_{0.119}]$ Core-Shell Nanofiller, *J. Am. Chem. Soc.*, 2012, **134**, 19099-19107.
6. M. A. Hickner, H. Ghassemi, Y. S. Kim, B. R. Einsla and J. E. McGrath, Alternative polymer systems for proton exchange membranes (PEMs), *Chem. Rev.*, 2004, **104**, 4587-4611.
7. E. Bakangura, L. Wu, L. Ge, Z. Yang and T. Xu, Mixed matrix proton exchange membranes for fuel cells: State of the art and perspectives, *Prog. Polym. Sci.*, 2016, **57**, 103-152.
8. M. Schuster, C. C. de Araujo, V. Atanasov, H. T. Andersen, K.-D. Kreuer and J. Maier, Highly Sulfonated Poly(phenylene sulfone): Preparation and Stability Issues, *Macromolecules*, 2009, **42**, 3129-3137.
9. K. D. Kreuer, A. Rabenau and W. Weppner, Vehicle Mechanism, A New Model for the Interpretation of the Conductivity of Fast Proton Conductors, *Angew. Chem.-Int. Edit. Engl.*, 1982, **21**, 208-209.
10. M. Tuckerman, K. Laasonen, M. Sprik and M. Parrinello, Ab initio molecular dynamics simulation of the solvation and transport of hydronium and hydroxyl ions in water, *J. Phys. Chem.*, 1995, **99**, 5749-5752.
11. H. O. Takaya Ogawa, Takanori Tamaki and Takeo Yamaguchi, Non-humidified proton conduction between a Lewis acid–base pair, *Phys. Chem. Chem. Phys.*, 2013, **15**, 13814 - 13817.
12. K. D. Kreuer, On the complexity of proton conduction phenomena, *Solid State Ionics*, 2000, **136**, 149-160.
13. K. D. Kreuer, S. J. Paddison, E. Spohr and M. Schuster, Transport in proton conductors for fuel-cell applications: Simulations, elementary reactions, and phenomenology, *Chem. Rev.*, 2004, **104**, 4637-4678.
14. D. Marx, Proton transfer 200 years after von Grotthuss: Insights from ab initio simulations, *ChemPhysChem*, 2006, **7**, 1848-1870.
15. T. Ogawa, T. Aonuma, T. Tamaki, H. Ohashi, H. Ushiyama, K. Yamashita and T. Yamaguchi, The proton conduction mechanism in a material consisting of packed acids, *Chem. Sci.*, 2014, **5**, 4878-4887.

16. M. Tuckerman, K. Laasonen, M. Sprik and M. Parrinello, Ab initio molecular dynamics simulation of the solvation and transport of hydronium and hydroxyl ions in water, *J. Chem. Phys.*, 1995, **103**, 150-161.
17. M. E. Tuckerman, D. Marx, M. L. Klein and M. Parrinello, On the quantum nature of the shared proton in hydrogen bonds, *Science*, 1997, **275**, 817-820.
18. N. Agmon, The Grotthuss mechanism, *Chem. Phys. Lett.*, 1995, **244**, 456-462.
19. T. C. Berkelbach, H. S. Lee and M. E. Tuckerman, Concerted Hydrogen-Bond Dynamics in the Transport Mechanism of the Hydrated Proton: A First-Principles Molecular Dynamics Study, *Phys. Rev. Lett.*, 2009, **103**, 4.
20. T. Ogawa, K. Kamiguchi, T. Tamaki, H. Imai and T. Yamaguchi, Differentiating Grotthuss Proton Conduction Mechanisms by Nuclear Magnetic Resonance Spectroscopic Analysis of Frozen Samples, *Anal. Chem.*, 2014, **86**, 9362-9366.
21. T. Ogawa, H. Ohashi, T. Tamaki and T. Yamaguchi, Proton diffusion facilitated by indirect interactions between proton donors through several hydrogen bonds, *Chem. Phys. Lett.*, 2019, **731**, 136627.
22. T. Ogawa, H. Ohashi, G. M. Anilkumar, T. Tamaki and T. Yamaguchi, Suitable acid groups and density in electrolytes to facilitate proton conduction, *Phys. Chem. Chem. Phys.*, 2021, **23**, 23778-23786.
23. N. Y. Abu-Thabit, S. A. Ali and S. M. Javaid Zaidi, New highly phosphonated polysulfone membranes for PEM fuel cells, *J Membrane Sci*, 2010, **360**, 26-33.
24. C. Alter, B. Neumann, H.-G. Stammler and B. Hoge, Synthesis and characterization of a novel highly phosphonated water-insoluble polymer, *J. Appl. Polym. Sci.*, 2020, **137**, 48235.
25. N. Fukuzaki, K. Nakabayashi, S. Nakazawa, S. Murata, T. Higashihara and M. Ueda, Highly phosphonated poly(N-phenylacrylamide) for proton exchange membranes, *J. Polym. Sci. Part A: Polym. Chem.*, 2011, **49**, 93-100.
26. J. M. Troup and A. Clearfield, On the Mechanism of Ion Exchange in Zirconium Phosphates. 20. Refinement of the Crystal Structure of α-Zirconium Phosphate, *Inorg. Chem.*, 1977, **16**, 3311-3314.
27. G. Alberti and M. Casciola, Composite membranes for medium-temperature PEM fuel cells, *Ann. Rev. Mater. Res.*, 2003, **33**, 129-154.
28. G. Alberti, M. Casciola, U. Costantino and R. Vivani, Layered and pillared metal(IV) phosphates and phosphonates, *Adv. Mater.*, 1996, **8**, 291-303.
29. G. Alberti, U. Costantino, F. Marmottini, R. Vivani and P. Zappelli, Zirconium Phosphite (3,3′,5,5′-Tetramethylbiphenyl)diphosphonate, a Microporous, Layered, Inorganic–Organic Polymer, *Angew. Chem. Int. Ed. Engl.*, 1993, **32**, 1357-1359.
30. G. M. Anilkumar, S. Nakazawa, T. Okubo and T. Yamaguchi, Proton conducting phosphated zirconia-sulfonated polyether sulfone nanohybrid electrolyte for low humidity, wide-temperature PEMFC operation, *Electrochem. Commun.*, 2006, **8**, 133-136.
31. A. Jayswal and U. Chudasama, Synthesis and characterization of a novel metal phosphonate, zirconium (IV)-hydroxy ethylidene diphosphonate, and its application as an ion exchanger, *Turk. J. Chem.*, 2008, **32**, 63-74.

32. H. Patel and U. Chudasama, A comparative study of proton transport properties of zirconium(IV) phosphonates, *Bull. Mat. Sci.*, 2006, **29**, 665-671.
33. R. Dragone, P. Galli, M. A. Massucci and M. Trombetta, Preparation and characterisation of histidine- and iron-histidine- alpha-zirconium phosphate intercalation compounds. Catalytic behaviour of the iron derivatives in oxidation reactions with H_2O_2, *J. Mater. Chem.*, 2003, **13**, 834-840.
34. Y. Sone, P. Ekdunge and D. Simonsson, Proton conductivity of Nafion 117 as measured by a four-electrode AC impedance method, *J. Electrochem. Soc.*, 1996, **143**, 1254-1259.
35. Y. Oshiba, J. Tomatsu and T. Yamaguchi, Thin pore-filling membrane with highly packed-acid structure for high temperature and low humidity operating polymer electrolyte fuel cells, *J. Power Sources*, 2018, **394**, 67-73.
36. A. Cabeza, M. d. M. Gómez-Alcántara, P. Olivera-Pastor, I. Sobrados, J. Sanz, B. Xiao, R. E. Morris, A. Clearfield and M. A. G. Aranda, From non-porous crystalline to amorphous microporous metal(IV) bisphosphonates, *Microporous Mesoporous Mat.*, 2008, **114**, 322-336.
37. J. L. Colón, D. S. Thakur, C.-Y. Yang, A. Clearfield and C. R. Martini, X-ray photoelectron spectroscopy and catalytic activity of α-zirconium phosphate and zirconium phosphate sulfophenylphosphonate, *J. Catal.*, 1990, **124**, 148-159.
38. V. Luca, J. J. Tejada, D. Vega, G. Arrachart and C. Rey, Zirconium(IV)-Benzene Phosphonate Coordination Polymers: Lanthanide and Actinide Extraction and Thermal Properties, *Inorg Chem*, 2016, **55**, 7928-7943.
39. E. Matczak-Jon, K. Slepokura, W. Zierkiewicz, P. Kafarski and E. Dabrowska, The role of hydrogen bonding in conformational stabilization of 3,5,6-and 3,5-substituted (pyridin-2-yl)aminomethane-1,1-diphosphonic acids and related (pyrimidin-2-yl) derivative, *J. Mol. Struct.*, 2010, **980**, 182-192.
40. S. H. Choi, J. N. R. Collins, S. A. Smith, R. L. Davis-Harrison, C. M. Rienstra and J. H. Morrissey, Phosphoramidate End Labeling of Inorganic Polyphosphates: Facile Manipulation of Polyphosphate for Investigating and Modulating Its Biological Activities, *Biochemistry*, 2010, **49**, 9935-9941.
41. T. Ogawa, T. Tamaki and T. Yamaguchi, Proton Conductivity of Organic–Inorganic Electrolyte for Polymer Electrolyte Fuel Cell, *Chem. Lett.*, 2017, **46**, 204-206.
42. R. Schmidt, E. W. Hansen, M. Stocker, D. Akporiaye and O. H. Ellestad, Pore Size Determination of MCM-51 Mesoporous Materials by means of ^{1}H NMR Spectroscopy, N_2 adsorption, and HREM. A Preliminary Study, *J. Am. Chem. Soc.*, 1995, **117**, 4049-4056.
43. N. Hara, H. Ohashi, T. Ito and T. Yamaguchi, Rapid Proton Conduction through Unfreezable and Bound Water in a Wholly Aromatic Pore-Filling Electrolyte Membrane, *J. Phys. Chem. B*, 2009, **113**, 4656-4663.
44. T. Ogawa, H. Ushiyama, J. M. Lee, T. Yamaguchi and K. Yamashita, Theoretical Studies on Proton Transfer among a High Density of Acid Groups: Surface of Zirconium Phosphate with Adsorbed Water Molecules, *J. Phys. Chem. C*, 2011, **115**, 5599-5606.
45. S. Takamuku, A. Wohlfarth, A. Manhart, P. Räder and P. Jannasch, Hypersulfonated polyelectrolytes: preparation, stability and conductivity, *Polym. Chem.*, 2015, **6**, 1267-1274.

46. S.-S. Bao, G. K. H. Shimizu and L.-M. Zheng, Proton conductive metal phosphonate frameworks, *Coord. Chem. Rev.*, 2019, **378**, 577-594.